

# ENHANCED RADAR DETECTION BY COMPRESSED SENSING CO-PROCESSING

*Srinivasan Kannan\**     *Han Lun Yap†*     *Justin Dauwels\**

\*School of Electrical & Electronic Engineering, Nanyang Technological University, Singapore – 639798.

†Sensors Division, DSO National Laboratories, Singapore –118226.

E-mail: srinivasan.sivam@gmail.com, yhanlun@dso.org.sg, jdauwels@ntu.edu.sg

## ABSTRACT

In radar systems, the target scene is typically reconstructed by matched filtering (MF). In the scenario of air surveillance, the target scene is usually sparse, and in such context, compressed sensing (CS) is applicable and potentially useful. We propose a novel detector for radar systems that utilizes both MF and CS reconstructions. More specifically, it applies the traditional constant false-alarm rate (CFAR) detector to a mixture of the MF and CS reconstructions. We test the proposed detector on data obtained from a monostatic radar that is illuminating commercial airliners. Results show that the proposed detector improves the target lock-in time by 25% compared to the MF-based CFAR detector at a given false-alarm rate of  $10^{-9}$ . It is noteworthy that the proposed method can readily supplement standard radar signal processing methods without modifications. Indeed, the CS reconstruction is implemented as a parallel processing branch, and the fusion procedure combines the standard radar reconstruction with the CS reconstruction, followed by standard CFAR detection.

**Index Terms**— compressed sensing, data fusion, CFAR detection, pulse-Doppler radar

## 1. INTRODUCTION

One primary interest in any active sensing applications is obtaining a representation of the target scene from noisy measurements. In radar, delay and Doppler shifts are important measurements obtained from the reconstructed target scene. In this paper, we first focus on obtaining a robust estimate of the range-Doppler plane and then analyse how this estimate can help in improving target detection. Here, we consider airborne targets where manoeuvring, acceleration, and off-grid positioning cause the reflected energy to spread, thereby reducing its signal-to-noise ratio (SNR); this in turn reduces the reliable detection of targets. Our interest lies in improving the reliability of target detection in the above-mentioned scenarios. We try to accomplish this with a supplement to matched filtering by compressed sensing (CS) reconstruction. Target tracking and identification will yield a considerable improvement even for a small improvement in the detection. In other

words, the supplementary information provided by the CS reconstruction can improve the usability of the measured data mostly by improving the detection in low SNR scenarios.

In this paper, we consider a collocated mono-static, far-field, and narrowband radar setup. Any complex target can be modelled by multiple point targets in the target plane, an assumption that holds well in most real-life scenarios. Conventionally the range-Doppler plane is obtained by matched filtering (MF), which is usually followed by a detector. In air surveillance scenarios, a low-resolution chirp-based radar is often used to search a large range swath ( $> 50$  km). In such scenarios, the number of air targets is very small compared to the data collected in the front end.

The theory of compressed sensing can be employed in different constructs [1] to address various radar signal processing problems. The fundamental problem of reliable target scene reconstruction from compressive measurements often requires a higher SNR [2]. Most other studies in CS radar [3–5] aim to reduce the sampling rate, which often leads to reduced detection performance. Although applications of CS in radar are interesting [1,2], practical applications remain limited, and a satisfactory operating regime still needs to be investigated.

Target detection with compressed measurements is an attractive issue addressed in [6], but it is effective only at high SNR scenarios due to the undersampling. CS-based detectors are proposed in [7] for high-resolution step-frequency radar scenario but without compromising the transmitted power. Some other studies [8,9] indicate that CS based detectors are not reliable for low values of false alarm probabilities. An initial attempt to control the false alarm probability by regularisation parameter in Lasso is studied theoretically in [10]. So far it has not been clearly proved that the performance of CS based detectors is better compared to conventional constant false-alarm rate detectors.

For mission critical applications, CS-based methods cannot yet be used as stand-alone techniques [11]. However, CS-based methods may be helpful as supplement to traditional radar systems to improve the overall performance. In our earlier study [12], we introduced an abstract framework to improve the sparse reconstruction of the radar target scene with guidance from matched filtering. In this paper, we propose

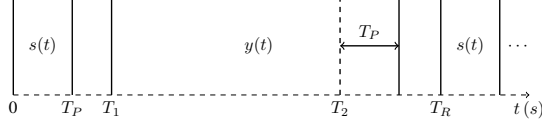


**Fig. 1.** Illustration of single-pulse transmit and return windows.

a practical approach to combine both MF and CS detectors. Particularly, we use the CS reconstruction as supplementary information to amplify selective pixels in the MF reconstruction. Subsequently, we analyse the effect of this fusion on target detection in a CFAR detector scenario.

In Section 2, we explain the problem setup and elaborate on range-Doppler reconstruction by matched filtering (MF) and by compressed sensing. In Section 3, we present the proposed fusion of MF and CS reconstruction and analyse how it enhances target detection. In Section 4, we present numerical results. In Section 5, we offer concluding remarks.

## 2. RANGE-DOPPLER RECONSTRUCTION

An illustration of the single-pulse radar transmit-and-return window is shown in Fig. 1. The probing signal is denoted by  $s(t) \in [0, T_P]$  and the radar return in the receive window is denoted by  $y(t) \in [T_1, T_2 + T_P]$ . Assuming  $L$  point targets in the target scene, the single-pulse radar return  $y(t)$  can be represented as:

$$y(t) = \sum_{i=1}^L \alpha_i s(t - \tau_i) + n(t), \quad (1)$$

where  $\alpha_i$  and  $\tau_i$  refer to the reflectivity coefficient and delay of the  $i^{\text{th}}$  target, respectively, and  $n(t)$  refers to circular white Gaussian noise. Denoting the bandwidth of  $s(t)$  by  $B_s$ , the sampled version of  $y(t)$  can be expressed in matrix form as  $\mathbf{y} = \mathbf{S}\mathbf{x} + \mathbf{n}$ , where  $\mathbf{S} \in \mathbb{C}^{(N+L) \times N}$ ,  $\mathbf{x} \in \mathbb{C}^{N \times 1}$ , and  $\mathbf{n} \in \mathbb{C}^{(N+L) \times 1}$  refer to delay matrix, delay profile, and noise vector, respectively. The matrix  $\mathbf{S}$  contains the sampled probing signal  $s(t)$  as columns separated by delays in multiples of  $\Delta t = 1/F_s$ , where  $F_s$  refers to the sampling rate. In radar systems, the returns over multiple pulses are used to improve the SNR by the process of integration over the ensemble. The moving targets introduce a phase (or Doppler) shift in the radar returns (see (1)); applying the Fourier transform cancels the acquired phase and provides the integration gain. Considering  $D$  radar-returns, the Fourier transform is computed over the  $D$  time points across the return ensemble. Representing  $D$  successive radar returns as columns of the matrix  $\mathbf{Y} = [\mathbf{y}_1 \ \mathbf{y}_2 \ \cdots \ \mathbf{y}_D]$ , the desired estimate of the delay-Doppler matrix  $\hat{\mathbf{X}} \in \mathbb{C}^{N \times D}$  is connected to  $\mathbf{Y}$  by the following equation:

$$\mathbf{Y}\mathbf{F} = \hat{\mathbf{S}}\hat{\mathbf{X}}, \quad (2)$$

**Input:** Measurement matrix  $\mathbf{S}_Q$ , measurements  $\mathbf{U} = \mathbf{Y}\mathbf{F}$ , sparsity  $K$   
**Output:**  $K$ -sparse approximation  $\mathbf{A}$  of the delay-Doppler plane  $\hat{\mathbf{X}}_{CS}$   
**Initialise:**  $\mathbf{A}^0 \leftarrow \mathbf{0}$ ;  $\mathbf{V} \leftarrow \mathbf{U}$ ;  $n \leftarrow 0$ ;  
**repeat**  
      $n \leftarrow n + 1$   
      $\mathbf{R} \leftarrow \mathbf{S}_Q^H \mathbf{V}$  /\* signal proxy \*/  
      $(\Omega_R, \Omega_D) \leftarrow \text{supp}(\mathbf{R}_K)$  /\*  $K$  element support \*/  
     **for each unique Doppler frequency** ( $d \in \Omega_D$ ) **do**  
          $\mathbf{B}(\Omega_R, d) = \mathbf{S}_Q^{\dagger}(:, \Omega_R) \mathbf{V}(:, d)$  /\* L-S estimate \*/  
      $\mathbf{B}(\Omega_R^c, \Omega_D^c) \leftarrow \mathbf{0}$   
      $\mathbf{C} \leftarrow \mathbf{B} + \mathbf{A}^{n-1}$  /\* merge \*/  
      $\mathbf{A}^n \leftarrow \mathbf{C}_K$  /\* prune \*/  
      $\mathbf{V} \leftarrow \mathbf{U} - \mathbf{S}_Q \mathbf{A}^n$  /\* update \*/  
**until** stopping criteria is met

**Fig. 2.** Compressive Sampling Matching Pursuit (CoSaMP) algorithm for delay-Doppler estimation. The original algorithm in [13] is modified to adequately support a sparse delay-Doppler estimate.

where  $\mathbf{F}$  refers to a  $D \times D$  Fourier matrix. The matrix  $\mathbf{F}$  performs focusing, and  $\mathbf{Y}\mathbf{F}$  represents the focused radar returns corresponding to  $D$  unambiguous Doppler frequencies. As can be seen from (1), ideally the estimate  $\hat{\mathbf{X}}$  should satisfy the constraint  $\|\hat{\mathbf{X}}\|_0 = L$ , where  $\|\cdot\|_0$  refers to the number of nonzeros in  $\hat{\mathbf{X}}$ . The matched filtering estimate of the range-Doppler plane, denoted by  $\hat{\mathbf{X}}_{MF}$ , is given by:

$$\hat{\mathbf{X}}_{MF} = \mathbf{S}^H \mathbf{Y}\mathbf{F}. \quad (3)$$

### 2.1. CS reconstruction of range-Doppler plane

In air-surveillance scenarios, often there are very few targets against the wide sky. Hence the number of constituent point targets, referred to as  $L$  in (1), is very small compared to the size of the delay-Doppler matrix  $\hat{\mathbf{X}} \in \mathbb{C}^{N \times D}$ , i.e.,  $L \ll ND$ . The solution for sparse delay-Doppler matrix,  $\hat{\mathbf{X}}$  in (2), can also be obtained by compressed sensing reconstruction algorithms. We apply compressive sampling matching pursuit (CoSaMP) [13] to solve for  $\hat{\mathbf{X}}$ ; the pseudo-code for the algorithm is listed in the Fig. 2. We solve the sparse matrix estimation problem with delays smaller than  $\Delta t$ ; the matrix  $\mathbf{S}$  can be modified to consider time-delays smaller than  $\Delta t$  by a factor  $Q$  [14]. Reducing the time-delay  $\Delta t$  by a factor  $Q \in \mathbb{Z}^+$  to  $\Delta t_Q = \Delta t/Q$ , we obtain the following system of equations:

$$\mathbf{Y}\mathbf{F} = \mathbf{S}_Q \hat{\mathbf{X}}_{CS}, \quad (4)$$

where  $\mathbf{S}_Q \in \mathbb{C}^{(N+L) \times QN}$  refers to the delay matrix and  $\hat{\mathbf{X}}_{CS} \in \mathbb{C}^{QN \times D}$  refers to the sparse estimate delay-Doppler matrix with the delay-profile enhanced in resolution by a factor  $Q$ . The system of equations represented by (4) is under-determined, and can be solved by CoSaMP for a  $K$ -sparse estimate  $\hat{\mathbf{X}}_{CS}$ .

We are interested in a typical two-hypothesis radar detection scenario, where for every cell of the range-Doppler plane, we need to decide whether or not a target is present. Instead of formulating a detection scheme exclusively in  $\hat{\mathbf{X}}_{MF}$  or  $\hat{\mathbf{X}}_{CS}$ , we will merge both reconstructions as discussed in Section 3.

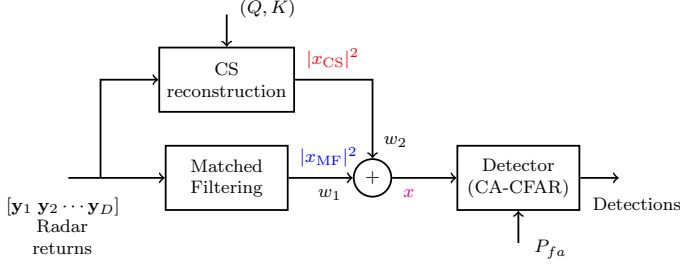


**Fig. 3.** Fusion of matched filtering and compressed sensing reconstruction.  $|x_{MF}|^2$  and  $|x_{CS}|^2$  refers to the power of the pixels in the corresponding range-Doppler reconstructions.

### 3. FUSION OF MF AND CS RECONSTRUCTIONS

The rationale behind the fusion of matched filtering ( $\mathbf{X}_{MF}$ ) and compressed sensing ( $\mathbf{X}_{CS}$ ) outputs is to obtain a delay-Doppler reconstruction that leads to improved target detection. We consider mixing  $\mathbf{X}_{MF}$  and  $\mathbf{X}_{CS}$  in a linear fashion:

$$\mathbf{X} = w_1 |\mathbf{X}_{MF}|^2 + w_2 |\mathbf{X}_{CS}|^2, \quad (5)$$

where  $w_1$  and  $w_2$  are positive weights that sum to unity; equation (5) represents an element-wise weighted squared sum of  $\mathbf{X}_{MF}$  and  $\mathbf{X}_{CS}$  to yield  $\mathbf{X}$ . An illustration of the fusion process is shown in Fig. 3. In this work, we aim to develop a CS-based detector similar to CFAR framework. Therefore, we set the weight  $w_2 > 95\%$  so that mostly the CS output is taken into account in the fused detector. The MF provides an estimate of the local noise, where the proposed detector inherits strategy similar to CFAR. As  $\mathbf{X}_{CS}$  is sparse, the fusion selectively emphasises a few elements in the range-Doppler plane. In Section. 3.2, we analyse the effect of fusion on target detection.

#### 3.1. CFAR detection

In realistic scenarios, the noise statistics vary over time and the Doppler dimension. Consequently, it is common to calculate the noise statistics locally in a window around the cell-under-test (CUT; see Fig. 4(b)). Cell averaging (CA) is a widely used method to estimate the noise power in a square-law detector [15]. Let  $N_r$  be the number of cells in the reference window. The noise power  $\hat{\beta}^2$  is calculated as follows:

$$\hat{\beta}^2 = \frac{1}{N_r} \sum_i |x_i|^2, \quad (6)$$

where  $x_i$  refers to the delay-Doppler estimate in the reference window. The threshold  $T$  is obtained as a function of the noise as  $T = \alpha \hat{\beta}^2$ . The scaling factor  $\alpha$  helps to ensure a fixed probability of false alarm  $P_{fa}$ , according to the following equation:  $\alpha = N_r (P_{fa}^{-1/N_r} - 1)$ . The estimated detection

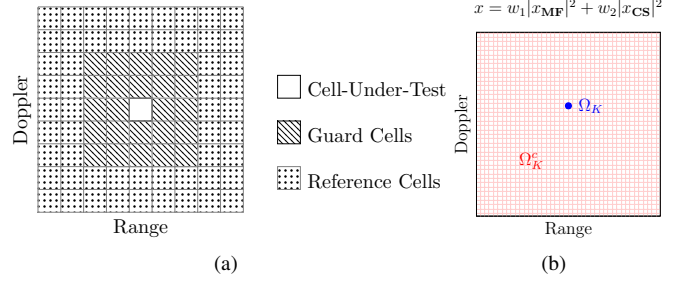


**Fig. 4.** Illustration of the fusion in delay-Doppler plane and its relevance to the CFAR detection. (a) Typical CFAR detection scenario, where we are concerned about the cases where CUT coincides with  $\Omega_K$ . (b) Fusion occurs only in the set  $\Omega_K$  where  $x_{CS} \neq 0$ , whereas in the complement set  $\Omega_K^c$  the value of  $x_{MF}$  is scaled by  $w_1$ .

probability is given by:

$$P_d = \left( 1 + \frac{\alpha}{N_r(1 + \chi)} \right)^{-N_r}, \quad (7)$$

where  $\chi$  refers to the SNR of the CUT with respect to the reference noise estimate. In the next section, we derive the detection probability of the detector operating on the fused reconstruction (5).

#### 3.2. Effect of the fusion on the SNR

We provide a visual illustration of the fusion in Fig. 4(a). The matrix  $\mathbf{X}_{CS}$  is a sparse estimate, and hence the process of fusion only affects particular locations in  $\mathbf{X}$  while the other elements only undergo scaling by  $w_1$ . We define the set  $\Omega_K$  as the locations where both terms in (5) are present, and the set  $\Omega_K^c$  as its complement where the first term in (5) is nonzero and the second term is zero.

In most cases, the elements in the set  $\Omega_K$  are isolated and surrounded by the elements from the complement set  $\Omega_K^c$ . We are interested in studying the improvement in SNR of the points in  $\Omega_K$  compared to  $\Omega_K^c$ , which is motivated by the CFAR detector where CUT or Guard Cells fall inside  $\Omega_K$  and the reference cells in its complement. From the above explanation, all the elements in the set  $\Omega_K^c$  have the following property:  $x_{\Omega_K^c} = w_1 x_{MF}^2$ , where scaling leads to a reduction in the amplitude in the set  $\Omega_K^c$  by a factor of  $w_1$ . By contrast, the elements in the set  $\Omega_K$  contain an additional term  $w_2 x_{CS}^2$  due to the CS reconstruction. The elements  $x_{CS}$  in the set  $\Omega_K$  are obtained by least-squares estimation by the CoSaMP algorithm. It can be shown that any non-zero element  $x_{CS}$  is related to  $x_{MF}$  by a positive constant  $w_c$ , and hence we can write  $x_{CS}^2 = w_c x_{MF}^2$ . Using the above relation, any element in the set  $\Omega_K$  is given by:  $x_{\Omega_K} = w_1 x_{MF}^2 + w_2 w_c x_{MF}^2 = (w_1 + w_2 w_c) x_{MF}^2$ . The relative improvement in the SNR is therefore given by the following scaling factor :

$$\chi_I = \frac{x_{\Omega_K}}{x_{\Omega_K^c}} = 1 + \frac{w_2}{w_1} w_c \in [1, \infty). \quad (8)$$

As scaling factor  $\chi_I \geq 1$ , it improves the original SNR, thereby always leading to an improvement in the detection probability  $P_d$  (7).

#### 4. RESULTS AND DISCUSSION

We evaluated the CFAR detector based on MF and the proposed fused detector on the real-life data. We set the CFAR detection threshold 13.2 dB above the local noise estimate; this corresponds approximately to a false-alarm rate of  $10^{-9}$  [15] for a Swerling 0 target. The data is acquired by a radar setup that is illuminating a commercial airliner manoeuvring to make a landing; data is recorded for a period of nearly 220 s. The probing waveform  $s(t)$  is a chirp signal with sufficient range resolution to distinguish point targets approximately no less than ten meters apart. We process data from  $D = 1024$  consecutive radar returns, which is referred to as a frame. To manage the computational complexity, we divide the entire receive window into smaller windows of size 15 km. We performed the processing on a MacPro workstation with an 2.6 GHz Intel Xeon processor and 16 GB of RAM.

We investigate here how the proposed fused detector can help in improving the tracking performance. We devised a simple tracking algorithm that predicts the location of the chosen target in the next frame by means of its Doppler and range value in the current frame. Detection is then performed in a sufficiently large window to accommodate possible target fluctuations. Finally, the tracking algorithm checks consistency of the detections across time and removes isolated detections; a particular detection is consistent only when two detections are present in four consecutive frames.

The tracking algorithm is initialised and monitored by the user to ensure its correctness. Our main objective here is to assess the performance of detection from a tracking perspective. Therefore, we decided to test the proposed and standard CFAR detector with a simple first-order tracking algorithm. The same methodology can be extended to more sophisticated tracking schemes. We apply CFAR detection on matched filtering (MF-CFAR) and the proposed fused detector, and the tracking algorithm operates on the resulting target detections. The range information provided by the tracking algorithm serves as a quantitative measure to assess the performance of the detectors.

The range information provided by the tracking algorithm using matched filtering CFAR detection and the proposed fused detector is shown in Fig. 5(a) and (b), respectively. The gaps in the tracks in Fig. 5(a) indicate that the target is not detected for brief periods of time. The gaps are primarily caused by the reduced SNR due to target acceleration and manoeuvring, interference, and fluctuating noise levels. In Fig. 5(b), we give the range information by the proposed detector with weights  $(w_1, w_2) = (0.1\%, 99.9\%)$ . As mentioned earlier, we choose a large value of  $w_2$ , since we aim to develop a CS based detector within the CFAR framework.

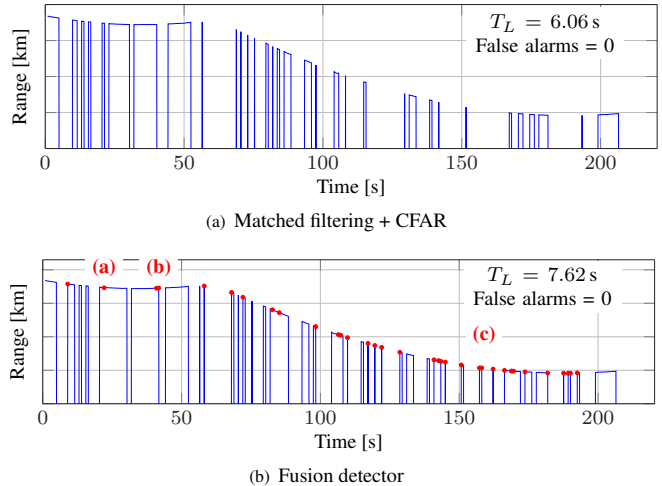


**Fig. 5.** Range information of the target from the tracking algorithm using MF-CFAR detector (top) and the proposed fused detector (bottom) in real-life data. The brief gaps indicate that the target is not detected in that time period. The additional detections from fusion are marked as red dots in (b). Each tick in  $y$ -axis corresponds to 1 km.

The additional detections provided by the proposed fused detector are marked as red dots along the track. The effect of the additional detections on the tracking performance is three-fold in comparison with MF-CFAR detector: gaps in the tracks are reduced, the tracks are extended, and new tracks are formed. Examples of these three effects are marked in red in Fig. 5(b), and indicated by (a), (b), and (c), respectively. These additional detections lead to an increased average length of individual tracks of the particular target; the track length is displayed in the top right corner of Fig. 5. The target lock-in time is improved by 25.6% compared to the MF-CFAR detector.

#### 5. CONCLUSION

In this paper, we presented a novel and practical radar detector that blends matched filtering and compressed sensing. We provided a theoretical derivation of the expected improvement in target SNR and detection probability of the proposed fused detector. Numerical experiments were conducted on real-life radar data. In this study, the proposed fused detector improved the target visibility by nearly 25% compared to matched filtering based detector at the same false-alarm rate. The approach proposed here can be readily implemented in existing air surveillance radar systems.

#### Acknowledgements

The research described in this paper is a part of the Project NURTURER funded by TL@NTU (Ref. no. TL-9012100777-04).

## 6. REFERENCES

- [1] L. C. Potter, E. Ertin, J. T. Parker, and M. Çetin, "Sparsity and compressed sensing in radar imaging," *Proc. of the IEEE*, vol. 98, no. 6, pp. 1006–1020, Jun. 2010.
- [2] J. Ender, "On compressive sensing applied to radar," *Signal Proc.*, vol. 90, pp. 1402 – 1414, 2010.
- [3] W. U. Bajwa, K. Gedalyahu, and Y. C. Eldar, "Identification of parametric underspread linear systems and super-resolution radar," *IEEE Trans. on Sig. Proc.*, vol. 59, no. 6, pp. 2548–2561, Jun. 2011.
- [4] L. Anitori, M. Otten, W. Van Rossum, A. Maleki, and R. Baraniuk, "Compressive CFAR radar detection," in *Radar Conference (RADAR), 2012 IEEE*, 2012, pp. 0320 – 0325.
- [5] O. Bar-Ilan and Y. C. Eldar, "A doppler focussing approach to sub-Nyquist radar," in *IEEE ICASSP 2013*, 2013, pp. 6531 – 6535.
- [6] M. A. Davenport, P. T. Boufounos, M. B. Wakin, and R. G. Baraniuk, "Signal processing with compressive measurements," *IEEE Trans. Sig. Proc.*, vol. 4, no. 2, pp. 445 – 460, Apr. 2010.
- [7] L. Anitori, A. Maleki, M. Otten, R. G. Baraniuk, and P. Hoogeboom, "Design and analysis of compressed sensing radar detectors," *IEEE Trans. in Sig. Proc.*, vol. 61, no. 4, pp. 813 –827, Feb. 2013.
- [8] L. Anitori and P. Hoogeboom, "False alarm probability estimator for compressed sensing radar," in *Radar Conference (RADAR), 2011 IEEE*, 2011, pp. 206 – 211.
- [9] M. C. Shastry, R. M. Narayanan, and M. Rangaswamy, "Characterizing detection thresholds using extreme value theory in compressive noise radar imaging," in *Compressed sensing II, 87170B*, ser. Proc. SPIE, F. Ahmad, Ed., vol. 8717, 2013, pp. 1 – 9.
- [10] H. L. Yap and R. Pribić, "False alarms in multi-target radar detection within a sparsity framework," in *International Radar conference*, Oct. 2014, pp. 1 – 6.
- [11] D. McMorrow, "Compressive sensing for DoD sensor systems," JASON, The MITRE Corporation, Tech. Rep., 2012.
- [12] J. Dauwels and K. Srinivasan, "Improved compressed sensing radar by fusion with matched filtering," in *IEEE Int. Conf. on Acoustics, Speech and Signal Processing*, May 2014, pp. 6795 – 6799.
- [13] D. Needell and J. A. Tropp, "CoSaMP: Iterative signal recovery from incomplete and inaccurate samples," *Appl. Comput. Harmon. Anal.*, vol. 26, pp. 301–321, 2009.
- [14] L. Zegov, R. Pribić, and G. Leus, "Waveform optimization for compressive sensing radar system," in *Workshop on Compressed sensing applied to radar (CoSeRa 2013)*, 2013, pp. 1–4.
- [15] M. A. Richards, *Fundamentals Of Radar Signal Processing*. McGraw-Hill Education Pvt. Limited, 2005.